Fuel xxx (2014) xxx–xxx

Contents lists available at ScienceDirect

Fuel

journal homepage: www.elsevier.com/locate/fuel

Kinetic study of the nopol synthesis by the Prins reaction over tin impregnated MCM-41 catalyst with ethyl acetate as solvent

Daniel Casas-Orozco, Edwin Alarcón, Aída Luz Villa *

Environmental Catalysis Research Group, Engineering Faculty, Chemical Engineering Department, Universidad de Antioquia UdeA, Calle 70 No. 52-21, Medellín, Colombia

HIGHLIGHTS

- The nopol rate model with ethyl acetate was the same that with toluene as solvent.
- Adsorption constants of compounds involved in the reaction were determined.
- Non-ideality of the liquid phase was related with the solvent solvation capacity.
- Solubility of formaldehyde in ethyl acetate was higher than in toluene.

GRAPHICAL ABSTRACT

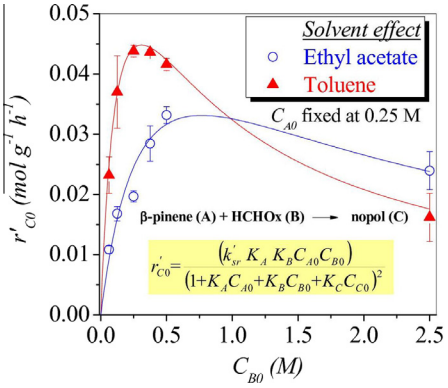

ARTICLE INFO

Article history:
Received 16 March 2014
Received in revised form 21 August 2014
Accepted 26 August 2014
Available online xxxx

Keywords:
Nopol
Sn-MCM-41
Prins reaction
Kinetic model
Solvent effect

ABSTRACT

The kinetics of the catalytic synthesis of nopol from β-pinene and paraformaldehyde over Sn-MCM-41 catalyst and using ethyl acetate as solvent is presented and compared with previous studies in toluene. Reaction rate data were fitted to a kinetic expression based on the Langmuir–Hinshelwood formalism, using the initial rates method. Reaction rate constant and adsorption constants were determined by regression of experimental data. The highest adsorption constant for nopol respect to reactants (K_C = 14.948 M^{-1}) allows to explain the strong inhibition effect of this compound that is experimentally observed. Solvent effects were discussed in terms of formaldehyde solubility, solvation of activated complex and reactants, and competitive adsorption on active sites. Higher solubility of formaldehyde in ethyl acetate respect to toluene, determined with Henry's law, along with the competitive adsorption of solvent and a more probable solvation of β-pinene and nopol may explain the better selectivity in ethyl acetate. Dependency of reaction constant on temperature was evaluated between 75 °C and 90 °C, resulting in an apparent activation energy of 98 kJ mol^{-1}, which is higher than in toluene, suggesting stabilization of carbocation intermediates by solvation in the polar ethyl acetate solvent.

1. Introduction

Nopol, 2-(7,7-dimethyl-4-bicyclo [3.1.1] hept-3-enyl) ethanol, is an added-value chemical synthesized through Prins reaction between paraformaldehyde and β-pinene, Fig. 1 [1]. This alcohol is used in household products formulations, agrochemicals, detergents and soaps [2]. β-Pinene, its natural precursor, is one of the main constituents of turpentine oil [3].

Several processes based on stoichiometric acid catalysts have been used traditionally for nopol synthesis: a homogeneously catalyzed reaction at 115–120 °C with zinc chloride to yield 57%

* Corresponding author. Tel.: +57 (4) 2196609.
E-mail address: aida.villa@udea.edu.co (A.L. Villa).

http://dx.doi.org/10.1016/j.fuel.2014.08.067
0016-2361/

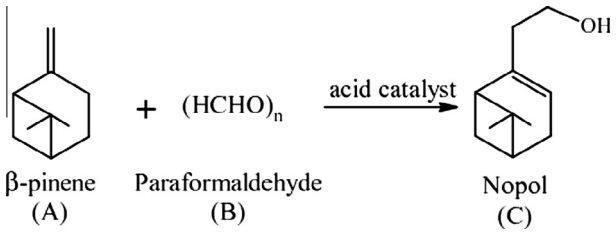

Fig. 1. Reaction scheme of Prins condensation between β-pinene and paraformaldehyde.

nopol, autoclaving a mixture of β-pinene and paraformaldehyde at 150–230 °C and reacting β-pinene and paraformaldehyde in the presence of acetic acid to obtain nopyl acetate, which is then saponified to nopol [4]. Some drawbacks arise from the aforementioned methods, as their low selectivity to nopol, high energy demands, use of toxic and corrosive chemicals, disposal of complex chemical residues and the difficulty to separate the catalyst from reaction mixture [5]. For this reason, different types of heterogeneous catalysts for nopol production have been recently studied, such as mesoporous iron phosphate [6], iron-zinc double metal cyanide complexes [5], Sn-SBA-15 materials [4,7], MWW-type zeolites [2], sulfated zirconia [8] and Sn-MCM-41 materials [9].

Nopol synthesis over Sn-MCM-41 mesoporous materials has advantages such as high selectivity towards nopol, high β-pinene conversion, simple catalyst synthesis procedure and possibility of catalyst recycling. Kinetic studies of nopol production over Sn-MCM-41 materials have been reported with toluene as solvent [10]. This study suggested that parallel reactions, such as isomerization of β-pinene and polymerization of formaldehyde in the gas phase, could decrease nopol yield. Ethyl acetate, which is less toxic and more selective to nopol production than toluene, inhibits the aforementioned undesired reactions [9,11]. Consequently, the kinetics of nopol production with ethyl acetate as solvent was studied in the composition ranges reported previously [10]. Comparison of the obtained kinetic parameters with the corresponding values in the case of toluene as solvent led to elucidate the effects of the solvent on the catalytic activity. Furthermore, temperature effects were studied between 75 and 90 °C.

2. Materials and methods

2.1. Catalyst synthesis

Tin-based material was synthesized by incipient wetness impregnation and characterized according to reported methods [9]. Briefly, for Sn-MCM-41 synthesis, 2 g of the mesoporous material support obtained following the method reported by Grun et al. [12] were put in contact with a solution of $SnCl_2 \cdot H_2O$ in ethyl acetate, added drop wise under inert atmosphere. The material was allowed to dry for 24 h and then calcined at 550 °C for 5 h.

2.2. Catalytic tests

Reactions were performed in 2 mL capped vials covered with silicone septas and under magnetic stirring at 2000 rpm (Fig. 2), to avoid external mass transfer limitations [10]. Catalytic tests were run in 6 batch reactors under identical conditions, i.e., 1 mg catalyst, 1 mL of β-pinene solution in ethyl acetate (0.0625–2.5 M) and paraformaldehyde powder (0.046–2.5 M). Reaction temperature was achieved by immersing the vials in an oil bath and controlled with an IKA fuzzy controller. Effect of reactants concentration on reaction rate of β-pinene and nopol was evaluated at 90 °C. Temperature effect was studied between 75 °C and 90 °C.

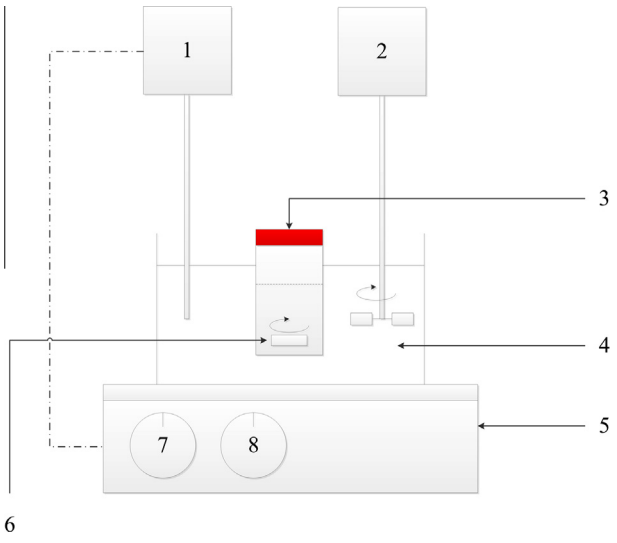

Fig. 2. Scheme of the experimental setup. 1: Temperature indicator and control, 2: mechanical stirrer, 3: capped vial, 4: oil bath, 5: heating plate, 6: magnetic stirrer, 7: temperature potentiometer, 8: stirring potentiometer.

Reactants and products were identified and measured using a GC–MS Agilent 7890 N, equipped with a DB-1 column, FID detector and autosampler. Calibration curves were obtained with dodecane as internal standard.

Reaction samples were withdrawn every 10 min and cooled immediately with pressurized air. Solid and liquid phases were separated by centrifugation. A catalyst particle size of 41.5 μm was used to avoid intraparticle mass transfer limitations, as reported in earlier studies [10]. Reaction rates were determined by taking the slope of the β-pinene or nopol concentration in the liquid phase as a function of time at $t = 0$. The reported reaction rates correspond to the average of at least two experiments.

3. Results and discussion

3.1. Internal mass transfer limitations

Table 1 shows the experimental concentration of reactants and observed rates for initial rate measurements. Weisz–Prater parameter, C_{WP}, Eq. (1) [13], was used as a criterion to detect intraparticle mass transfer limitations for both β-pinene and formaldehyde [14,15].

Table 1
Initial reaction rate data as a function of the concentration of β-pinene (*A*), paraformaldehyde (*B*) and nopol (*C*) in ethyl acetate as solvent.

Run	C_{i0} (mol/L)			r_{i0} (mol g^{-1} h^{-1})		SD (mol g^{-1} h^{-1})	
	A	*B*	C	$-r'_{A0}$	r'_{C0}	$-r'_{A0}$	r'_{C0}
1	0.250	0.063	0	0.01396	0.01085	0.00196	0.00066
2	0.250	0.125	0	0.01979	0.01679	0.00238	0.00118
3	0.250	0.250	0	0.02455	0.01966	0.00295	0.00093
4	0.250	0.375	0	0.03507	0.02845	0.00264	0.00296
5	0.250	0.500	0	0.04292	0.03318	0.00493	0.00139
6	0.250	2.500	0	0.01846	0.02394	0.00571	0.00316
7	0.063	0.250	0	0.01034	0.00702	0.00123	0.00063
8	0.125	0.250	0	0.02155	0.01394	0.00192	0.00067
9	0.375	0.250	0	0.03708	0.03188	0.00301	0.00172
10	0.500	0.250	0	0.04806	0.03962	0.00234	0.00255
11	1.000	0.250	0	0.04454	0.03685	0.00491	0.00143
12	2.500	0.250	0	0.08911	0.03630	0.00789	0.00186
13	0.463	0.046	0	0.01868	0.01139	0.00268	0.00125
14	0.250	0.250	0.0625	0.02186	0.01248	0.00246	0.00138
15	0.250	0.250	0.125	0.00963	0.00325	0.00122	0.00064

Please cite this article in press as: Casas-Orozco D et al. Kinetic study of the nopol synthesis by the Prins reaction over tin impregnated MCM-41 catalyst with ethyl acetate as solvent. Fuel (2014), http://dx.doi.org/10.1016/j.fuel.2014.08.067

$$C_{WP} = -r_{A0}^{exp} R^2 \rho_p / (D_{eff,i} C_{i,s}) \quad (1)$$

with $-r_{A0}^{exp}$: observed initial reaction rate for β-pinene, R: average catalyst particle radius (20.75 μm), ρ_p: catalyst particle density (2 g/cm^3), $D_{eff,i}$: effective diffusivity of reactant i in the solvent, $C_{i,s}$: concentration of reactant i at the catalyst surface. For first order reaction, values of $C_{WP} \ll 1$ are typically attributed to not significant concentration gradients existing within the catalyst particle [13]; however, a more precise criterion is $C_{WP} \leq 3\beta$, where β is the maximum decrease in concentration gradient in pores, which is function of the reaction order. β values of 0.1, 0.2 and 2 are estimated for second, first and zero order reaction, respectively [16]. Then, a conservative criteria for the absence of intraparticle mass transfer limitations is to consider $C_{WP} \leq 0.3$.

Diffusivity of β-pinene in ethyl acetate was estimated with Eq. (2), which is valid for molar fractions lower than 0.1 [16].

$$D_{12}^{0,l} = 4.4 \times 10^{-15} (T/\eta_2)(V_2/V_1)^{1/6} (L_2^{vap}/L_1^{vap})^{1/2} \quad (2)$$

with $D_{12}^{0,l}$: bulk diffusivity of diluted liquid solute 1 in a liquid solvent 2 (m^2/s); T: absolute temperature (K); η_2: dynamic viscosity of the solvent at the reaction temperature (Pa s); V: molar volume of each species at the reaction temperature (m^3 k mol^{-1}); L: latent heat of vaporization at normal boiling point (J k mol^{-1}). Physical properties were obtained from [17].

For mole fractions greater than 0.1 (Runs 11 and 12), β-pinene diffusivity was calculated using Eq. (3), which is useful for non-aqueous solvents [16].

$$D_{12} = (D_{21}^{0,l})^{x_1} (D_{12}^{0,l})^{x_2} / \eta_m \quad (3)$$

with D_{12}: bulk diffusivity of a concentrated liquid solute in a liquid solvent (m^2 s^{-1}), x_1: solvent molar fraction , x_2: solute molar fraction, η_m: viscosity of the mixture (Pa s), Eq. (4)

$$\eta_m = \Pi \eta_j^{x_j} \quad (4)$$

with η_j: viscosity of pure liquid j.

Formaldehyde diffusivity in the liquid phase was estimated using Eq. (5):

$$D_{12}^{0,g} = 1.1728 \times 10^{-16} T \sqrt{X M_2} / \eta_2 V_1^{0.6} \quad (5)$$

where $D_{12}^{0,g}$: bulk diffusivity of a dilute gas solute 1 in a liquid solvent 2 (cm^2/s), T: temperature (K), M_2: molecular weight of solvent, η_2: viscosity of solvent (Pa s), V_1: molar volume of the solute (m^3 kmol^{-1}), X: solvent association parameter ($X_{ethyl\ acetate}$ = 1 [16]).

Effective diffusivity of reactant i through catalyst pores was determined with Eq. (6) [16].

$$D_{eff,i} = D_i (1 - \lambda)/(1 + 16.26\lambda) \quad (6)$$

with D_i: bulk diffusivity of reactant i in the liquid mixture, λ: ratio of molecular size to the pore radius, that is obtained with Eq. (7) [16].

$$\lambda = \varphi_i / \varphi_p \quad (7)$$

where φ_i: molecular size of diffusing species i (Å), φ_p: mean pore diameter of catalyst (Å).

The Van der Waals radii were simulated in ACD/ChemSketch® freeware package, and the values obtained were 3.3 Å and 1.05 Å for β-pinene and formaldehyde, respectively. Pore diameter of catalyst was determined in previous studies, and its mean value was 20 Å (2 nm) [18]. Calculated diffusivities (Eqs. (2)–(7)), at 90 °C, are presented in Table 2.

Calculations of the Weisz–Prater criterion for β-pinene were obtained with its initial concentration. Formaldehyde monomer species concentration was obtained considering its production from paraformaldehyde depolymerization by thermal effects, according to an Avrami–Erofeyev model, Eq. (8) [11].

$$dN_{POM}/dt = -dN_f/dt = -2N_{POM} k^2 t \quad (8)$$

N_{POM}: moles of polymer, k: reaction rate constant for depolymerization (h^{-1}), t: time (h), N_f: total moles of formaldehyde in the system.

For this reason, certain time is required until the formaldehyde concentration in the liquid reaches a value such that the Weisz–Prater criterion is satisfied. According to previous studies [10], no external mass transfer limitations exist at the stirring rates used in the experimental runs; thus, gas–liquid equilibrium was assumed for formaldehyde and Henry's Law was used to estimate its liquid phase concentration [15]. A material balance leads to obtain an expression for describing formaldehyde concentration in the liquid phase as a function of time, Eq. (9)

$$dC_{f,l}/dt = dN_f/dt \cdot 1 \Big/ \left[V \cdot \left(1 + \frac{H_f \ V_{gas}}{RT \quad V} \right) \right] \quad (9)$$

where $C_{f,l}$: formaldehyde concentration in the liquid phase (M), V: reaction volume (mL), V_{gas}: volume of gas in the vial (mL), H_f: Henry's constant of formaldehyde in the liquid mixture (L atm^{-1} mol^{-1}), R: gas constant (L atm^{-1} mol^{-1} K^{-1}), T: reaction temperature (K).

H_f was estimated through a mixing rule, Eq. (10) [19].

$$\ln H_f = \sum x_j \ln H_{f,j} \quad (10)$$

with

Table 2
Calculated diffusivities of reactants in ethyl acetate as solvent (Eqs. (2)–(7)).

Run	Bulk diffusivity (cm^2/s × 10^6)		Effective diffusivity (cm^2/s × 10^6)	
	A	*B*	*A*	*B*
1	59.22	124.95	4.18	36.97
2	59.22	124.97	4.18	36.98
3	59.22	124.99	4.18	36.98
4	59.22	125.02	4.18	36.99
5	59.22	125.05	4.18	37.00
6	59.22	124.97	4.18	36.97
7	59.22	126.63	4.18	37.47
8	59.22	126.11	4.18	37.31
9	59.22	123.89	4.18	36.66
10	59.22	122.79	4.18	36.33
11	57.36	118.14	4.04	34.96
12	53.82	103.76	3.79	30.70
13	59.22	123.03	4.18	36.40
14	59.22	123.84	4.18	36.64
15	59.22	122.65	4.18	36.29

Table 3
Weisz-Prater criterion for β-pinene and formaldehyde in ethyl acetate and toluene.

Run	Ehtyl acetate			Toluene[b]		
	$C_{f,l}$ (M)[a]	$C_{W\text{-}P,A}$	$C_{W\text{-}P,B}$[a]	$C_{f,l}$ (M)[a]	$C_{W\text{-}P,A}$	$C_{W\text{-}P,B}$[a]
1	0.0100	0.032	0.090	0.0097	0.242	0.546
2	0.0199	0.045	0.064	0.0195	0.165	0.186
3	0.0398	0.056	0.040	0.0390	0.226	0.127
4	0.0596	0.080	0.038	0.0585	0.229	0.086
5	0.0795	0.098	0.035	0.0779	0.182	0.051
6	0.3975	0.042	0.003	0.3897	0.122	0.007
7	0.0397	0.094	0.017	0.0388	0.636	0.090
8	0.0397	0.099	0.035	0.0388	0.397	0.112
9	0.0398	0.057	0.061	0.0391	0.149	0.126
10	0.0399	0.055	0.079	0.0392	0.072	0.082
11	0.0073	0.026	0.076	na	na	na
12	0.0398	0.022	0.172	na	na	na
13	0.0398	0.023	0.168	0.0072	0.088	0.499
14	0.0401	0.050	0.036	0.0390	0.113	0.064
15	0.0404	0.022	0.016	0.0391	0.105	0.060

na: not measured.
[a] Estimated at 10 min of reaction.
[b] Calculated from experimental data in Ref. [10].

Please cite this article in press as: Casas-Orozco D et al. Kinetic study of the nopol synthesis by the Prins reaction over tin impregnated MCM-41 catalyst with ethyl acetate as solvent. Fuel (2014), http://dx.doi.org/10.1016/j.fuel.2014.08.067

$$H_{f,j} = \gamma_{f,j}^{\infty} P_f^{sat} M_j / \rho_j \quad (11)$$

where x_j: mol fraction of solvent j in the liquid mixture (j: β-pinene, ethyl acetate, nopol), $H_{f,j}$: Henry's constant of formaldehyde in the solvent j (L atm mol^{-1}); $\gamma_{f,j}^{\infty}$: activity coefficient at infinite dilution of formaldehyde in the solvent j (estimated in Aspen Plus® with UNIFAC-DMD model), M_j: molecular weight of the solvent j, ρ_j: density of solvent j (g L^{-1}), P_f^{sat}: saturation pressure of formaldehyde at the reaction temperature (atm).

Table 3 shows the calculated Weisz-Prater criterion for both β-pinene and paraformaldehyde in ethyl acetate and in toluene. In the case of formaldehyde, the Weisz–Prater criterion was calculated at the time of the first sample withdrawal, i.e. 10 min. In ethyl acetate, the Weisz–Prater criterion is satisfied for both β-pinene and formaldehyde; although in toluene higher values are obtained, it is still near or below the limit of 0.6 established for first order reactions.

3.2. Kinetic rate law

For initial rate calculations (Table 1), it is necessary to consider the depolymerization reaction to provide formaldehyde, and the Weisz–Prater criterion estimated in Section 3.1, which suggest the possibility of an induction period, due to a lack of available formaldehyde in the liquid phase for the reaction. Fig. 3 illustrates the expected dissolved formaldehyde, obtained from Eqs. (8)–(12) assuming no reaction. The steepest ascent is clear from 6 min, however, the inset figure indicates that at times as low as 6 s, the available formaldehyde in the liquid phase per gram of catalyst is above 24 μmol/g, the tin loading on MCM-41. According to kinetic curves (see Supplementary Tables s.1–s.4 and Fig. s.1) an induction period is not observed. In agreement with these explanations, the induction period could be obtained from the inverse of the turn over frequency (TOF) [16,20]. The measured TOF at initial rates ($TOF = r'_{i,0}/(tin\ loading\ in\ mol\ per\ gram)$) were in the range 0.122–1.05 s^{-1}, resulting on induction times of around 8 and 1 s, respectively. Summarizing, in spite of the implicit depolimerization step of paraformaldehyde, induction period was too short to be noticeable under the tested conditions.

Previous studies, in toluene as solvent [10], showed that the Prins reaction between β-pinene and paraformaldehyde over Sn-MCM41, Fig. 1, obeys a Langmuir–Hinshelwood mechanism, with the adsorption of reactants and products in equilibrium and the surface reaction as the rate-limiting step, Eq. (12)–(15).

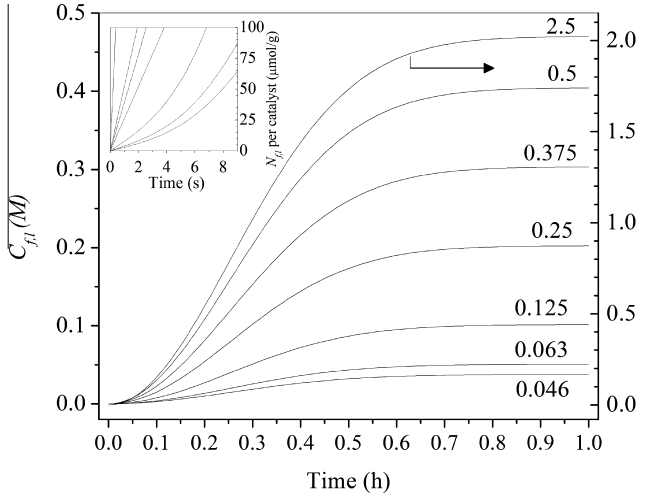

Fig. 3. Simulation of the *in situ* dissolved formaldehyde without reaction, N_f: moles of formaldehyde in the liquid.

$$A + S \overset{K_A}{\leftrightarrow} A \cdot S \quad (12)$$

$$B + S \overset{K_B}{\leftrightarrow} B \cdot S \quad (13)$$

$$A \cdot S + B \cdot S \overset{k'_{sr}}{\leftrightarrow} C \cdot S + S \quad (14)$$

$$C \cdot S \overset{K_C}{\leftrightarrow} C + S \quad (15)$$

Eq. (16) represents the dependency of reaction rate on the concentration of reacting and product species, according to the assumed reaction mechanism.

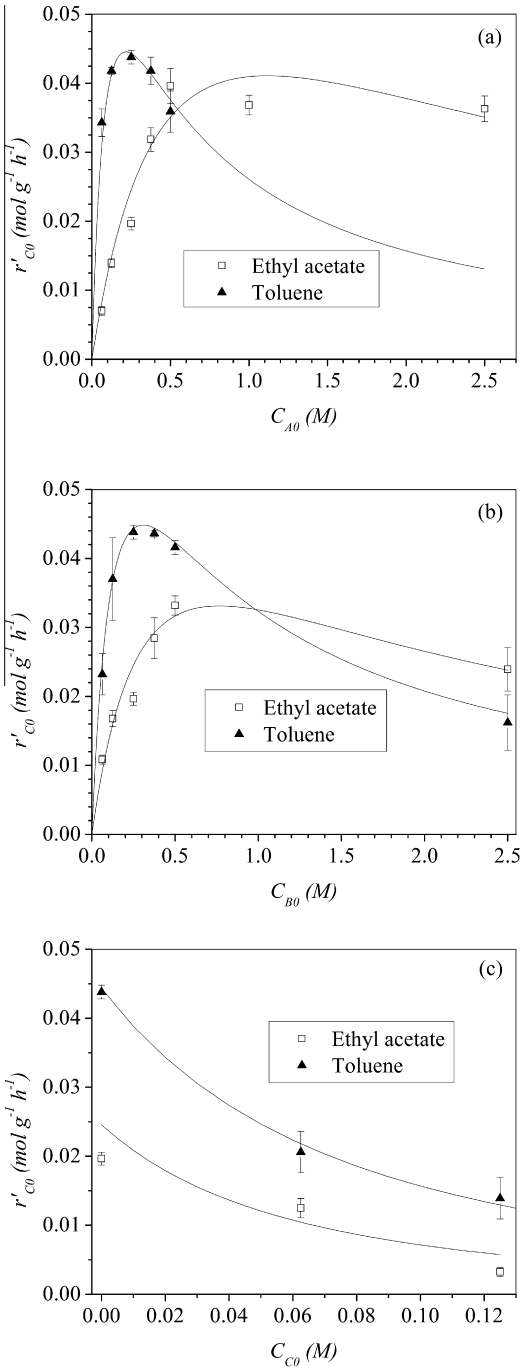

Fig. 4. Effect of initial concentrations of reactants on the initial reaction rate of nopol. (a) C_{A0} effect with C_{B0} = 0.25 M, C_{C0} = 0. (b) C_{B0} effect with C_{A0} = 0.25 M, C_{C0} = 0, (c) C_{C0} effect with C_{A0} = C_{C0} = 0.25 M. Experimental (▲, □) and predicted by Eq. (16) (continuous lines). Toluene data adapted from Ref. [10].

Please cite this article in press as: Casas-Orozco D et al. Kinetic study of the nopol synthesis by the Prins reaction over tin impregnated MCM-41 catalyst with ethyl acetate as solvent. Fuel (2014), http://dx.doi.org/10.1016/j.fuel.2014.08.067

$$r'_C = k'_{sr} K_A K_B C_A C_B / (1 + K_A C_A + K_B C_B + K_C C_C)^2 \quad (16)$$

where r'_C: reaction rate for nopol (mol g^{-1} h^{-1}), K_i: equilibrium adsorption constant for species i (M^{-1}), k'_{sr}: surface reaction constant (mol g^{-1} h^{-1}), C_i: concentration of species i (M).

In the absence of nopol (Table 1, runs 1–12), Fig. 4a and b shows a behavior consistent with previously reported data with toluene as solvent with a maximum reaction rate corresponding to bimolecular mechanism and Eq. (16) [10]. When nopol is added from the beginning of the reaction, the inhibition effect was also observed (Table 1, runs 3, 14 and 15, Fig. 4c) [10]. As the trend with ethyl acetate is the same that in the case of toluene, we could suggest that the proposed mechanism is consistent with experimental data.

In agreement with experiments at higher conversions [10], the reaction rates in ethyl acetate are lower than the values observed in toluene (Fig. 4). On the other hand, the maximum initial rate in toluene has been observed under equimolar concentrations of β-pinene and paraformaldehyde (0.25 M for both reactants, Fig. 4a and b), while an excess of either β-pinene or paraformaldehyde is required to obtain the maximum rate in ethyl acetate (Fig. 4a and b, respectively).

3.3. Data fitting

Kinetic model, Eq. (16), was fitted to experimental rate data of nopol formation, Table 1. Levenberg–Marquardt algorithm was used to minimize the sum of the squared error, Eq. (17).

$$SSE = \sum (r'^{exp}_{C0j} - r'^{calc}_{Cj})^2 \quad (17)$$

where r'^{exp}_{C0j}: observed initial reaction rate of nopol (mol g^{-1} h^{-1}), r'^{calc}_{C0j}: calculated initial reaction rate of nopol (mol g^{-1} h^{-1}).

Only nopol was assumed as product, because no chromatographic peaks related with byproducts were observed during the analyses performed on samples and its selectivity up to 9 h in ethyl acetate was above 90%, as reported earlier [9]. As nopol selectivity in ethyl acetate was close to selectivity reported in toluene, the same kinetic analysis was carried out in both ethyl acetate and toluene solvents [10].

The order of magnitude of the initial values used in the optimization routine was found by a sensibility analysis [21]. The parameters were initialized in a value of 1, and each one was changed, one at a time, to evaluate Eq. (16) at different orders of magnitude, Fig. 5. Initial values determined with this approach were $k'_{sr} = 10^0$, $K_A = 10^0$, $K_B = 10^0$, $K_C = 10^1$. Using these values, the optimization algorithm took 8 iterations to converge, with a squared error of 2.012×10^{-4}. Resulting parameters are summarized in Table 4. Fig. 6 shows a random distribution of the residuals, which confirms the validity of the solution.

In order to assure that the converged values correspond to an overall minimum for Eq. (17), a new sensibility analysis was performed. It consisted in calculating the response of the objective function to a perturbation in one parameter at a time letting the rest at their estimated values [21,22]. It can be seen from Fig. 7 that any variation of the parameter in the range ±20% causes an increase in the objective function. This indicates that the obtained solution corresponds to a global minimum.

Obtained parameters, along with the previously reported values with toluene as solvent, are shown in Table 4. Continuous lines in Fig. 4, indicates the good prediction of initial rates with the regressed parameters in the tested solvents. It is noticeable that nopol adsorption constant is an order of magnitude larger than the corresponding values for the reactants. This explains the behavior observed in Fig. 4c, where a strong inhibition effect is observed when nopol is added at the beginning of the reaction.

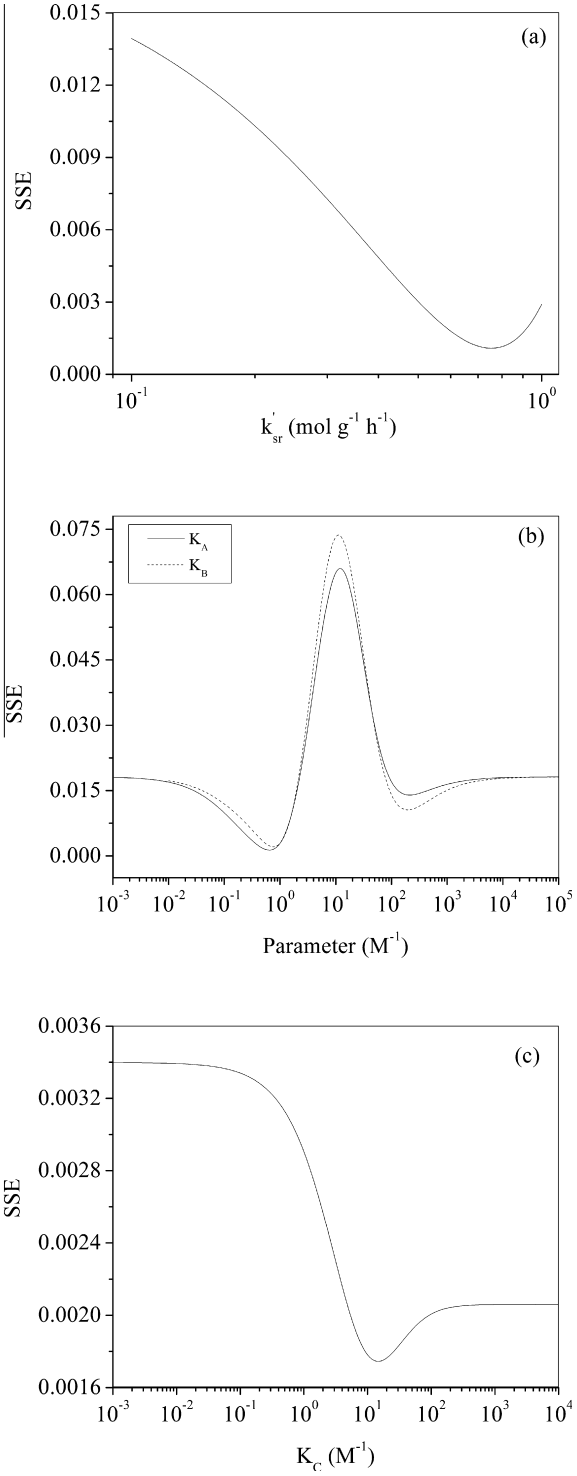

Fig. 5. Order of magnitude determination for the guess values in the optimization routine. (a) k'_{sr} with $K_A = K_B = K_C = 1$, (b) K_A with the found value of $k'_{sr} = 10^0$ and $K_B = K_C = 1$, (c) K_B with the found values of $k'_{sr} = 10^0, K_A = 10^0$ and $K_C = 1$, (d) K_C with the found values of $k'_{sr} = 10^0, K_A = 10^0, K_B = 10^0$.

Adsorption constant of formaldehyde is higher than β-pinene adsorption constant in ethyl acetate as solvent. The opposite tendency is observed in toluene as solvent. This is an indicative of a better stabilization of adsorbed formaldehyde molecules due to solvation by ethyl acetate [23], a relatively polar compound compared with toluene. However, since stronger solvation effects in the bulk liquid take place in ethyl acetate (Section 3.5) than in toluene, the net effect is a

Please cite this article in press as: Casas-Orozco D et al. Kinetic study of the nopol synthesis by the Prins reaction over tin impregnated MCM-41 catalyst with ethyl acetate as solvent. Fuel (2014), http://dx.doi.org/10.1016/j.fuel.2014.08.067

Table 4
Constants of Eq. (16) found by regression of experimental data.

Parameter	Solvent	
	Ethyl acetate	Toluene [10]
k'_{sr} (mol g^{-1} h^{-1}) ± SD	0.546 ± 0.082	0.185 ± 0.009
K_A (M^{-1}) ± SD	1.2804 ± 0.206	126.000 ± 35.0
K_B (M^{-1}) ± SD	1.7214 ± 0.331	105.000 ± 29.1
K_C (M^{-1}) ± SD	14.948 ± 6.758	400.600 ± 4 × 10^{-8}
R^2	0.950	0.918
MSE	7.7384 × 10^{-6}	1.2 × 10^{-5}

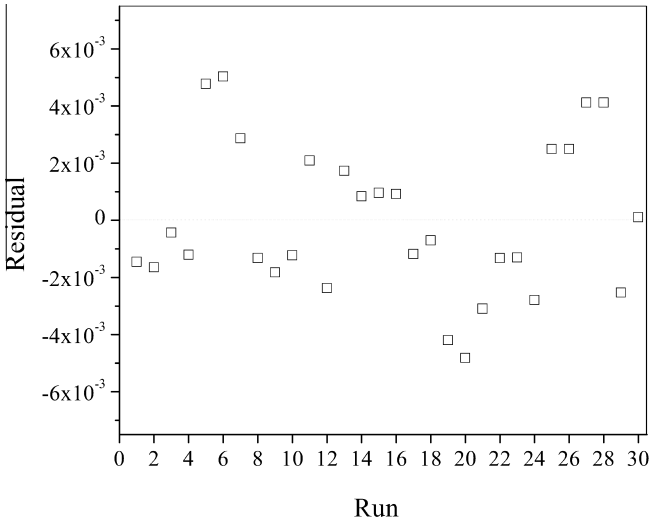

Fig. 6. Residual plot for the optimization results.

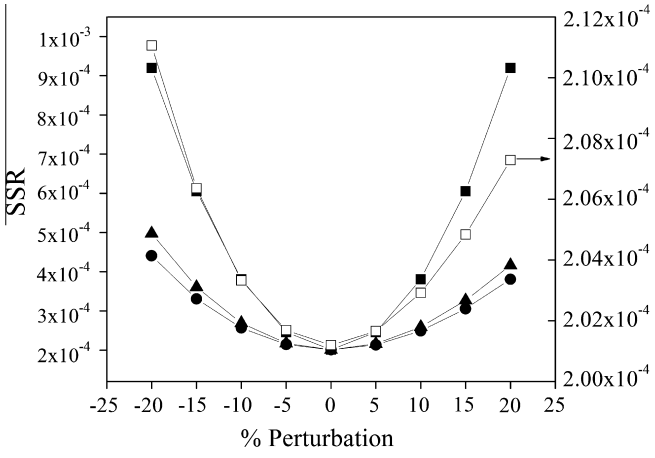

Fig. 7. Sensitivity analysis for the obtained solution after optimization routine (■: k'_{sr}, ●: K_A, ▲: K_B, □: K_C).

moderate higher adsorption of formaldehyde respect to β-pinene, even when it is present in a greater amount in the liquid phase, given its increased solubility in ethyl acetate.

Higher adsorption constants are found when the reaction is carried out with toluene as solvent. Liquid-phase non-idealities in ethyl acetate are presumed to be the cause of this behavior and are discussed in Section 3.5.

3.4. Temperature effect

The reaction rate was experimentally determined between 75 °C and 90 °C with $C_{A0} = C_{B0} = 0.25$ M and $C_{C0} = 0$, Table 5. No internal mass transfer limitations were detected when Weisz–Prater criterion was calculated (Table 6). Parameters describing the temperature effect on the reaction rate can be found with Eqs. (18) and (19) [24].

Table 5
Effect of temperature on production rate of nopol.

T (°C)	ln (r'_{c0})	SD
75	−5.3498	0.044
80	−4.7748	0.055
85	−4.4123	0.064
90	−3.9291	0.047

Reaction conditions: 1 mg catalyst, 1.0 mL of β-pinene in ethyl acetate solution, $C_{A0} = C_{B0} = 0.25$ M.

$$E_{app} = -R\, d(lnr'_{C0})/d(1/T) \quad (18)$$

$$lnA_{app} = E_{app}/RT + lnr'_{C0} \quad (19)$$

where E_{app}: apparent energy of activation (kJ mol^{-1}), and A_{app}: apparent pre-exponential factor (mol g^{-1} h^{-1}).

Reaction rate data at different temperatures, Table 5, were used to construct an Arrhenius plot, i.e., lnr'_{C0} vs. 1/T (Fig. 8), from which temperature parameters were found by linear regression. A_{app} and E_{app} were 2.63 × 10^{12} mol g^{-1} h^{-1} and 98 ± 5 kJ/mol, respectively. E_{app} is higher than observed values in toluene (E_{app} = 78 ± 9 kJ mol^{-1}) and thermal activated reaction (E_{app} = 79 ± 4 kJ mol^{-1}) [10]. Differences in the polarity of the solvents and E_{app} suggest the presence of an activated complex containing oppositely charged ions which are stabilized by solvation with the polar ethyl acetate [23]. The intermediate specie is more probably associated to the interaction of adsorbed formaldehyde on tin active sites, as schematized in the suggested mechanisms in previous studies [5,8,25]. Since, apparent activation energy deals with the difference between true activation energy and the enthalpies of adsorption for each compound, results suggest the greater contribution of adsorption phenomena when toluene is the solvent, resulting in the compensation effect described in this solvent [10].

3.5. Solvent effects

Solvent effect on conversion and nopol selectivity at long times has been related with polarity and paraformaldehyde solubility [9]. From kinetic point of view over heterogeneous catalysts, solvent effects could be assessed by: (i) the influence of mass transfer due to differences in diffusivity in the liquid, (ii) the gas solubility in the solvent (or liquid mixture), (iii) the non-ideality in liquid phase due to interactions of solvent and solute, and (iv) the competitive solvent adsorption on the catalyst surface [15]. Mass transfer resistances were discussed in Section 3.1. Although Weisz–Prater criteria trend to be higher in toluene than in ethyl acetate, catalytic activity in both ethyl acetate and toluene were carried out under kinetic regime. Solvent effects on adsorption and surface reaction constants, Table 4, and Arrhenius parameters are not explained by the mass transfer.

As indicated in Section 3.1, the reaction system involves a solubilized gas that diffuses through the pores and is adsorbed on active sites. Henry's constants in the mixtures containing toluene and ethyl acetate were 6.46 and 4.97 L bar mol^{-1}, respectively. These data confirm a higher solubility of formaldehyde in ethyl acetate than in toluene. As the competitive adsorption of reactants is a fact by the magnitude of their constants, a higher availability of formaldehyde in the liquid media could partially explain the best selectivity in ethyl acetate. Moreover, to consider the competitive

Please cite this article in press as: Casas-Orozco D et al. Kinetic study of the nopol synthesis by the Prins reaction over tin impregnated MCM-41 catalyst with ethyl acetate as solvent. Fuel (2014), http://dx.doi.org/10.1016/j.fuel.2014.08.067

Table 6
Evaluation of Weisz–Prater criterion for the runs at different temperatures.

T (°C)	$-r_{A0\ (obs)}$ (mol g^{-1} h^{-1})	SD (mol g^{-1} h^{-1})	$C_{B,l}$ (M)	Bulk diffusivity (cm^2/s × 10^6)		Effective diffusivity (cm^2/s × 10^6)		$C_{W\text{-}P}$	
				A	B	A	B	A	B
75	0.0084	0.0029	0.0170	51.16	108.62	3.61	32.14	0.022	0.037
80	0.0112	0.0068	0.0229	53.45	110.99	3.77	32.84	0.029	0.036
85	0.0153	0.0038	0.0300	55.84	113.42	3.94	33.56	0.037	0.036
90	0.0245	0.0030	0.0398	59.22	124.99	4.18	36.98	0.056	0.040

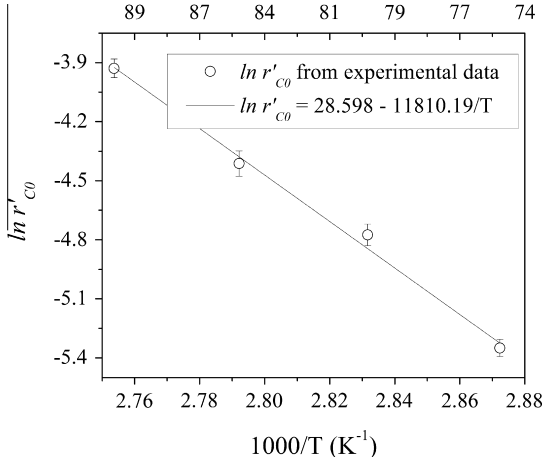

Fig. 8. Temperature dependency of surface reaction constant of nopol production in ethyl acetate.

adsorption of the solvent, Eq. (16) was modified with the adsorption constant of the solvent (K_{sol}), Eq. (20).

$$r'_C = k'_{sr}K_AK_BC_AC_B/(1 + K_AC_A + K_BC_B + K_CC_C + K_{sol}C_{sol})^2 \quad (20)$$

with C_{sol}: solvent concentration (M).

Parameters calculated for ethyl acetate by non-linear regression are shown in Table 7. Results indicate that ethyl acetate could be also adsorbed on active sites, but at lower extent compared to the reactants and the product. The corresponding adsorption constants of reactants and products are about ten times higher than the previous calculated values, Table 7, but they are still lower than in toluene. With toluene as solvent no consistent values were fitted from different starting points; for instance, K_{solv} was $-0.15 \pm 9.29 \times 10^{-5}$ M^{-1} or 0.0235 ± 3.15 M^{-1}. This suggests that toluene adsorption should be neglected from statistical point of view. The solvent polarity, determined with the normalized solvatochromic polarity parameter, E_T^N, is higher for ethyl acetate ($E_T^N = 0.288$) than for toluene ($E_T^N = 0.099$) [9,26]. High polarity of ethyl acetate causes a competitive adsorption on active sites on the catalyst surface, which is related with the lower adsorption constants of the reacting species with this solvent. Several authors have discussed these effects on heterogeneous catalyzed reactions. Jadhav et al. [8] studied the solvent effect on the catalytic condensation of β-pinene and paraformaldehyde over sulfated zinc ferrite catalysts. The authors related the increased polarity of the used non-protic solvents with the decrease in β-pinene conversion, due to competitive interaction of solvent lone electron pairs with Zn^{2+} Lewis acid sites on the catalyst surface, as in the case of acetonitrile solvent. D'Agostino et al. [27] studied the effect of water on the aerobic oxidation of 1,3-propanediols, using titania-supported gold catalysts. Using NMR techniques, the authors related the presence of water with an increased substrate-solvent interaction, which weakens the interaction of reagents with catalytic surface and makes the solvent to access selectively to catalyst surface.

As discussed in Section 3.4, probably the solvation effects are present in the transition state of nopol reaction mechanism, in which intermediate carbocations are formed as reacting species that are adsorbed on the acidic Lewis sites of the catalyst [5,23]. On the other hand, solvation also occurs in the bulk reactant molecules; these interactions hinder the reactants, preventing them to be adsorbed on catalyst surface. The relative strength of these phenomena dictates the overall effect of solvent–solute interactions on reaction rate. In the case of ethyl acetate, activity coefficients, Table 8, show that liquid-phase non-idealities are more pronounced in this solvent than in toluene, favoring the bulk solvation phenomenon [23]. This may explain the observed decrease in reaction rates in ethyl acetate, suggesting that bulk solvation is stronger than solvation effects on the intermediate adsorbed molecules.

These facts are confirmed by observing that at low concentrations of β-pinene – high solvent concentrations – (0.063 M < C_{A0} < 0.25 M, Fig. 4a), reaction rates are lower in ethyl acetate ($0.0076 < r'_{C0} < 0.020$ mol g^{-1} h^{-1}) than in toluene ($0.034 < r'_{C0} <$ 0.044 mol g^{-1} h^{-1}).

By decreasing solvent amount, reaction rate in ethyl acetate continues to grow in a broader range of concentration than in the case of toluene (with C_{B0} = 0.25 M and C_{C0} = 0), reaching a maximum in ethyl acetate with $C_{A0} = 0.5$ M ($r'_{C0} = 0.040 \pm 0.0026$ mol g^{-1} h^{-1}), while in toluene, the maximum reaction rate is observed at $C_A = 0.25$ M ($r'_C = 0.044 \pm 0.0010$ mol g^{-1} h^{-1}). Moreover, maximum reaction rate in ethyl acetate is 11% lower than the obtained velocity in toluene; however, this reduction is not as pronounced as the corresponding reduction in adsorption constants, possibly due to the increased solubility of formaldehyde in ethyl acetate. It is noteworthy that solubility of formaldehyde in the solvent is critical, since this compound is generating *in situ*, thus it is not available from the beginning of the reaction [27].

Table 7
Constants of Eq. (20) found by regression of experimental data in ethyl acetate, when the effect of the solvent adsorption is included.

Parameter	Value
k'_{sr} (mol g^{-1} h^{-1}) ± SD	0.493 ± 0.033
K_A (M^{-1}) ± SD	12.035 ± 0.852
K_B (M^{-1}) ± SD	14.586 ± 1.372
K_C (M^{-1}) ± SD	127.95 ± 27.98
K_{solv} (M^{-1}) ± SD	0.737 ± 4.11 × 10^{-7}
R^2	0.9501
MSE	8.048 × 10^{-6}

Table 8
Activity coefficients at infinite dilution in solvents.[a]

Solute	Solvent	
	Ethyl acetate	Toluene
β-Pinene	3.69	1.08
Nopol	5.67	2.90
Formaldehyde	1.76	2.24

[a] Estimation in Aspen Plus® with UNIFAC-Dortmund model.

Please cite this article in press as: Casas-Orozco D et al. Kinetic study of the nopol synthesis by the Prins reaction over tin impregnated MCM-41 catalyst with ethyl acetate as solvent. Fuel (2014), http://dx.doi.org/10.1016/j.fuel.2014.08.067

Increased selectivity towards nopol has been reported previously when ethyl acetate is used as solvent [9,10]. This can be attributed to the lower adsorption of β-pinene respect to paraformaldehyde in this solvent, which prevents β-pinene reactant from undergoing isomerization reactions [6], being β-pinene isomers the main byproducts for this reaction [9,10].

Furthermore, lower magnitude adsorption of nopol in this solvent can also prevent it from reacting to other products, increasing the selectivity towards the main product [28].

4. Conclusions

A reaction rate equation based on the Langmuir–Hinshelwood formalism was adjusted to nopol experimental initial reaction rates data with ethyl acetate as solvent. Similarly with previous studies in toluene, the mathematical adjustment showed that the proposed mechanism based on the dual-site model is consistent with experimental data. The higher solubility of formaldehyde in the liquid and adsorption capacity of the solvent could explain the best selectivity in ethyl acetate respect to toluene. Liquid-phase non-idealities are more pronounced in ethyl acetate than in toluene, and were related with higher solvation capacity of bulk species such as β-pinene and nopol. Apparent activation energy was 98 ± 5 kJ/mol, which is greater than the corresponding value in toluene (67 ± 10 kJ/mol). Differences in the apparent activation energy suggest stabilization by solvation of carbocation intermediates when the polar ethyl acetate is the solvent.

Acknowledgments

This work was supported by "Departamento Administrativo de Ciencias, Tecnología e Innovación COLCIENCIAS" Contract RC-0572-2012-Bio-Red-Co-CENIVAM and Universidad de Antioquia (UdeA) Sustainability Strategy 2013-2014. D.C. acknowledges to COLCIENCIAS his doctoral fellowship.

Appendix A. Supplementary material

Supplementary data associated with this article can be found, in the online version, at http://dx.doi.org/10.1016/j.fuel.2014.08.067.

References

[1] Pastor IM, Yus M. The Prins reaction: advances and applications. Curr Org Chem 2007;11:925–57.
[2] Wang J, Jaenicke S, Chuah GK, Hua W, Yue Y, Gao Z. Acidity and porosity modulation of MWW type zeolites for Nopol production by Prins condensation. Catal Commun 2011;12:1131–5.
[3] Coppen JJ, Hone GA. Gum naval stores: Turpentine and rosin from pine resin. Non-wood forest products 2. Food Agric Organ United Nations, 1995. p. 71.
[4] Selvaraj M, Choe Y. Well ordered two-dimensional SnSBA-15 catalysts synthesized with high levels of tetrahedral tin for highly efficient and clean synthesis of nopol. Appl Catal A Gen 2010;373:186–91.
[5] Patil MV, Yadav MK, Jasra RV. Prins condensation for synthesis of nopol from β-pinene and paraformaldehyde on novel Fe–Zn double metal cyanide solid acid catalyst. J Mol Catal A Chem 2007;273:39–47.
[6] Pillai UR, Sahle-Demessie E. Mesoporous iron phosphate as an active, selective and recyclable catalyst for the synthesis of nopol by Prins condensation. Chem Commun (Camb) 2004:826–7.
[7] Ramaswamy V, Shah P, Lazar K, Ramaswamy AV. Synthesis, characterization and catalytic activity of Sn-SBA-15 mesoporous molecular sieves. Catal Surv Asia 2008;12:283–309.
[8] Jadhav SV, Jinka KM, Bajaj HC. Nanosized sulfated zinc ferrite as catalyst for the synthesis of nopol and other fine chemicals. Catal Today 2012;198:98–105.
[9] Alarcón E, Correa L, Montes C, Villa AL. Nopol production over Sn-MCM-41 synthesized by different procedures – Solvent effects. Microporous Mesoporous Mater 2010;136:59–67.
[10] Villa AL, Correa LF, Alarcón E a. Kinetics of the nopol synthesis by the Prins reaction over tin impregnated MCM-41 catalyst. Chem Eng J 2013;215–216:500–7.
[11] Grajales E. Cinética de depolimerizacion de paraformaldehído y polimerización de formaldehído en fase gaseosa. Universidad de Antioquia; 2013.
[12] Grun M, Unger KK, Matsumoto A, Tsutsumi K. Novel pathways for the preparation of mesoporous MCM-41 materials : control of porosity and morphology. Microporous Mesoporous Mater 1999;27:207–16.
[13] Fogler S. Elements of Chemical Reaction Engineering. 4th ed. New York: Prentice Hall; 2006.
[14] Shekhawat D, Nagarajan K, Jackson JE, Miller DJ. Kinetics of citraconic anhydride formation via condensation of formaldehyde and succinates. Org Process Res Dev 2002;6:611–7.
[15] Mukherjee S, Vannice M. Solvent effects in liquid-phase reactions II. Kinetic modeling for citral hydrogenation. J Catal 2006;243:131–48.
[16] Vannice A. Kinetics of catalytic reactions. New York: Springer Science+Business Media, Inc.; 2005.
[17] Yaws CL. Yaws' handbook of thermodynamic and physical properties of chemical compounds. Knovel; 2003.
[18] Alarcón E. Síntesis de Nopol mediante la reacción de Prins con catalizadores heterogéneos. Universidad de Antioquia; 2010.
[19] Poling BE, Prausnitz JM, O'Connell J. The Properties of Gases and Liquids. 5th ed. United States: McGraw Hill; 2001.
[20] Boudart M, Djega-Mariadassou G. Kinetics of heterogeneous catalytic reactions. New Jersey: Prentice Hall; 1984.
[21] Alcázar LA, Ancheyta J. Sensitivity analysis based methodology to estimate the best set of parameters for heterogeneous kinetic models. Chem Eng J 2007;128:85–93.
[22] Jarullah AT, Mujtaba IM, Wood AS. Kinetic parameter estimation and simulation of trickle-bed reactor for hydrodesulfurization of crude oil. Chem Eng Sci 2011;66:859–71.
[23] Reichardt C, Welton T. Solvents and solvent effects in organic chemistry. 4th ed. Weinheim: Wiley-VCH; 2011.
[24] Lynggaard H, Andreasen A, Stegelmann C, Stoltze P. Analysis of simple kinetic models in heterogeneous catalysis. Prog Surf Sci 2004;77:71–137.
[25] Yang NC, Ding-Djung H, Ross C. The mechanism of the Prins reaction. J Am Chem Soc 1959;3450:1–4.
[26] Wypych G. Handbook of solvents. Toronto: ChemTec Publishing; 2001.
[27] D'Agostino C, Kotionova T, Mitchell J, Miedziak PJ, Knight DW, Taylor SH, et al. Solvent effect and reactivity trend in the aerobic oxidation of 1,3-propanediols over gold supported on titania: NMR diffusion and relaxation studies. Chemistry 2013;19:11725–32.
[28] Gilbert L, Mercer C. Solvent effects in heterogeneous catalysis: Application to the synthesis of fine chemicals. In: Delmon B, Yates JT, editors. Heterog. Catal. Fine Chem. III, Louvain: Elsevier; 1993, p. 51–66.